Dual-axis Lorentz Force MEMS Magnetometer

Aditi[1, 2], Supriyo Das[1], Prateek Kothari[1], Surajit Das[1] and Ram Gopal[1,2]
Smart Sensor Area,
[1]CSIR-Central Electronics Engineering Research Institute (CEERI),
Pilani-333031, India
[2]Academy of Scientific and Innovative Research (AcSIR),
Ghaziabad- 201002, India
Email: aditi.ceeri@gmail.com

***Abstract*—This paper presents a dual axis MEMS magnetometer, utilizing two DOF torsional gyroscope structure. The designed structure is a torsional resonator with two gimbals. A single structure can detect magnetic field in two directions. The first and second mode of vibrations are the desired mode of operation for detecting the magnetic field in x and y directions. The first and second modes of vibrations are at 107 kHz and 187 kHz respectively. The device is tested for its Lorentz force transduction using MSA-500 in the presence of magnetic field generated using permanent magnet for both the axes at atmospheric pressure. The fabrication process is based on anodic bonding (<400°C) of a borofloat glass wafer and double side polished (DSP) Si wafer, which enables the passivation between Gold loop and Silicon.**

Keywords*— *Dual-axis, LDV, Lorentz Force, Magnetometer, Torsional

I. INTRODUCTION

Over the last decade, magnetometers have been extensively used in consumer electronics applications for multifunction devices, automotive industry, and non-destructive material testing [1]. Its demand in portable gadgets like watches and mobile phones are increasing as they are useful in orientation and navigation applications [2]. The dominant technologies used for medium to high sensitivity portable applications are magneto-resistive, Hall Effect and Fluxgate sensors [3]. However, MEMS Lorentz force based sensors are grabbing attention as it has the benefit of easy integration with other inertial sensors like accelerometers and gyroscope [4,7]. It does not require any specialized magnetic material unlike magneto-resistive magnetic sensors, thus can be fabricated by standard MEMS processes. MEMS magnetometers have better sensitivity as compared to Hall Effect sensors [5]. The available fluxgate sensors are relatively difficult to fabricate and have poor scaling properties [6]. In the current technological context, MEMS technology can be used to develop sensors which are small in size, consume low power, are easy to fabricate, offer better resolution and are of low cost. Currently accelerometers and gyroscopes are integrated using MEMS processes. Hall Effect and anisotropic magneto-resistance (AMR) are dominant technologies used in IMUs and conventional magnetometers are based on these technologies. AMR sensors require specialized magnetic material and therefore suffer from hysteresis and are sensitive to in-plane fields [7]. For sensing out-of-plane fields, the sensor needs to be vertically packaged hence require large volume. Whereas, Hall Effect sensors consume high power for desired sensitivity and offer low resolution w.r.t. AMR sensors. Therefore, Lorentz force based MEMS sensor can be an alternative with low power consumption and better resolution.

Most of the magnetic sensors detect magnetic field in one direction[8-10]. It is of paramount importance to design and develop sensors such that a single sensor can detect magnetic field in more than one direction. Thereby chip size can be reduced, leading to smaller packages[11-14]. Two axis sensors, using single structure reported [13-14] are for x/y and z magnetic field detection. For x and y direction magnetic field sensing, these sensors require two separate sensors to be placed perpendicular to each other. In this article we report a dual axis magnetic sensor which is designed such that a single sensor can sense magnetic field in x and y direction, without the need of switching [2] the direction of current flow. A two DOF torsional gyroscope structure has been utilized for dual axis magnetometer for the first time. It has been fabricated using standard anodic bonding technique for realizing the device which is relatively easy in fabricating the device and require low temperature processes (<400°C). It enables easy addition of passivation layer between the multi-loop gold coil (0.8 μm) and silicon which reduces the need of serpentine elements to join the loops w.r.t existing three axis [11] monolithic structures. Due to the existing passivation layer in the present device, the maximum current flow may be enhanced based on the required sensitivity. A torsional two axis magnetic sensor is designed, fabricated and tested for its operation and is described in the following sections.

II. DEVICE DESCRIPTION

The torsional resonator utilizes rotational vibratory motion for its resonant modes. The dual axis sensing is implemented with an out-of-plane motion about x-axis and the other out-of-plane motion about y-axis. Fig.1. depicts the schematic of the proposed torsional magnetometer. The overall structure is composed of two masses: outer gimbal and inner gimbal. The anchors are placed at the extreme ends of the outer gimbal by beams along x-axis. The outer gimbal is free to oscillate about x-axis. The inner gimbal oscillates with the outer about x-axis and also oscillates independently about y-axis with proper Lorentz force actuation. Two bottom electrode plates are placed underneath the inner gimbal and other two beneath the outer gimbal. The oscillation detection of inner and outer gimbal by capacitive sensing mechanism can be detected by the electrodes placed below.

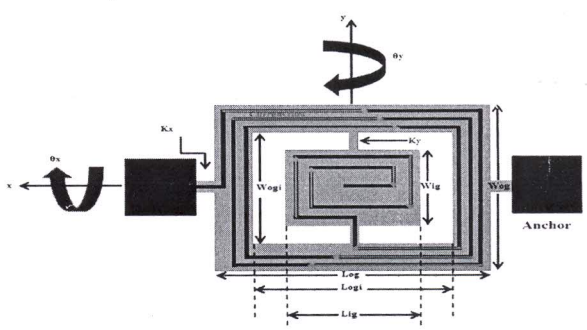

Fig.1. Conceptual schematic of the proposed torsional MEMS magnetometer structure

When an excitation current is applied in the coil and the external magnetic field is applied in y direction, Lorentz force is produced and the outer gimbal along with inner resonates in out-of plane direction. In addition, if the magnetic field is applied in x-direction, the inner gimbal introduces Lorentz force and hence the displacement occurs in out-of-plane direction. Presently, the displacement is measured using Laser Doppler Vibrometry (LDV). A capacitive sensing circuit could be used to measure the change in capacitance due to the vibration magnitude using the bottom electrodes placed on glass cavity. The equations of motion about x-axis and y-axis of the magnetometer by conservation of angular momentum subjected to an external magnetic field with small angle approximation is given as follows,

The equation of motion along x-axis may be written as,

$$(I_x^{og} + I_x^{ig})\,\ddot{\theta_x} + (D_x^{og} + D_x^{ig})\dot{\theta_x} + K_x^{og}\theta_x = M_{mo}, \quad (1)$$

The equation of motion along y-axis may be written as,

$$I_y^{ig}\ddot{\theta_y} + D_y^{ig}\dot{\theta_y} + K_y^{ig}\theta_y = M_{mi}, \quad (2)$$

I_x^{og} and I_x^{ig} are the respective moment of inertia (I) of the outer and inner gimbals about x-axis; I_y^{og} is the moment of inertia of the outer gimbal about y-axis; D_x^{og} and D_x^{ig} are the respective damping coefficients about x-axis associated with outer and inner gimbal; D_y^{ig} is the damping coefficient in y-direction related to inner gimbal; K_x^{og} is defined for the springs for motion across x-axis; K_y^{ig} is defined for the springs for motion across y-axis; θ_x and θ_y are angle of deflections across x and y axis; M_{mo} and M_{mi} is the Lorentz force moment applied to actuate the gimbals when external magnetic field is applied; $I_x \sin(\omega t)$ is the sinusoidal excitation current applied with frequency ω and B_y is the external magnetic field for motion along y-axis; $I_y \sin(\omega t)$ is the sinusoidal excitation current applied with frequency ω and B_x is the external magnetic field for motion along x-axis. Using 1 and 2, the device design parameters were calculated as shown in Table I.

TABLE I. DEVICE DESIGN PARAMETERS

Parameter	Value (μm)
Thickness of Si (t)	15
Outer gimbal length (Log)	510
Outer Gimbal width (Wog)	360
Inner gimbal length (Lig)	300
Inner gimbal width (Wig)	150
Outer spring length	21
Outer spring width	14.5
Inner spring length	25
Inner spring width	11.5
Holes	8 x 8

III. FABRICATION

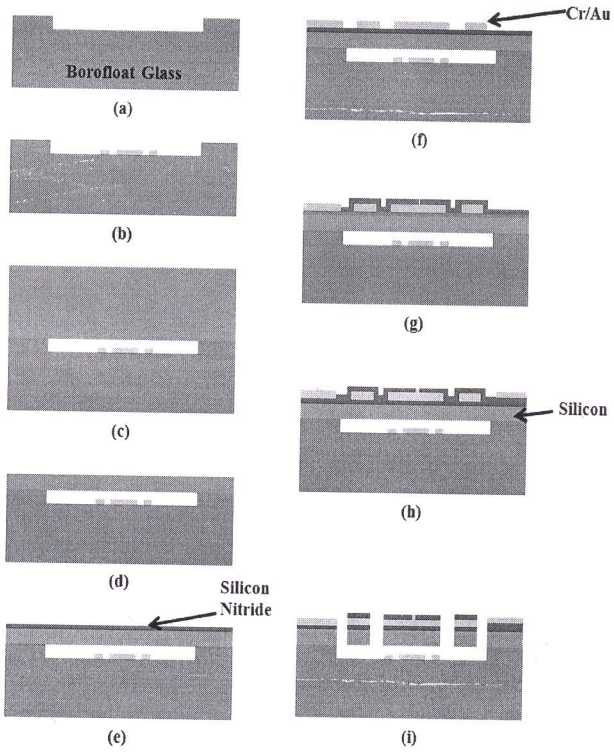

Fig.2. Fabrication process flow (a)Borofloat glass etching (0.9 μm) (b) Cr/Au(200 Å /2000 Å) sputter deposition and patterning (c) Anodic bonding (d) TMAH etching of silicon (e) PECVD Silicon Nitride deposition (0.4 μm) (f) Cr/Au (200 Å / 8000 Å) sputter deposition and patterning of coil (g) PECVD Silicon Nitride deposition and patterning (0.4 μm) (h) Cr/Au(200 Å /2000 Å) sputter deposition and patterning of top contact (i) Patterning of structure and RIE of Silicon Nitride(0.8 μm) and DRIE (15μm) Silicon

The fabrication process is based on 6 levels of mask. Initially the borofloat wafer is etched for a depth of ~0.9 μm for cavity formation. The depth is measured using Dektak profiler. Fig.2 (a) shows the optical image of the cavity formed with anchors. Thereafter, patterning of bottom electrode and contact pad is performed as depicted in Fig.2 (b). Next, the borofloat wafer and Si wafer is anodic bonded as depicted in Fig.2(c). Thereafter the Si wafer is bulk micro-machined to a thickness of 15 ± 5 μm using wet etching with TMAH as shown in Fig.2 (d). The etching has been monitored continuously as there is no etch stop layer. The thickness was measured using measurement gauge. Then, PECVD Silicon Nitride of 0.4 μm is deposited on the wafer as passivation, shown in Fig.2 (e). This step is followed by deposition of Cr/Au of 200 Å / 8000 Å thicknesses and then patterning for coil formation as depicted in Fig.2 (f). Next, again PECVD Nitride (0.4 μm) is deposited on the wafer and patterned for taking the coil contact as delineated in Fig.2 (g). Fig.2 (h) shows the patterned and etched Nitride showing the gold layer of the below formed coil. Thereafter, Cr/Au of 200 Å/ 2000 Å is patterned for the top contact as depicted in Fig.2 (h). Later, the device is patterned using positive PR using Mask 6. Then, the passivation layer (0.4 μm + 0.4 μm) of Nitride is etched using RIE. After Nitride etching, silicon layer is etched using DRIE for final release of the device as shown in Fig.2 (i). At last the positive photoresist is removed using Plasma stripper

d the wafer is diced to chips. Fig.3 (a,b) shows the SEM icrographs of the released sensor and its tilted view.

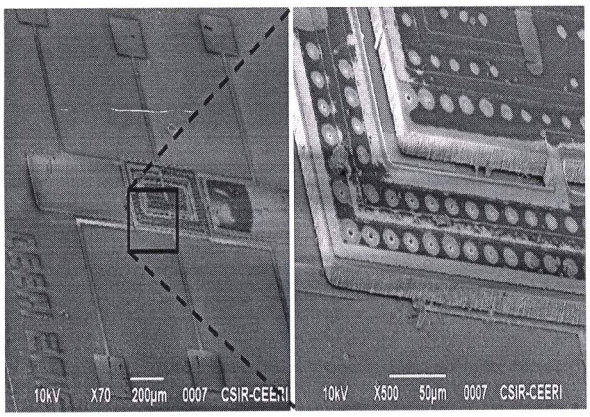

(a) (b)

Fig.3. SEM micrographs (Fabricated Magnetometer- top view (b) Tilted view of the fabricated dual axis MEMS Magnetometer

IV. RESULTS AND DISCUSSION

The released device was characterized using Polytec-Micro System Analyser (MSA-500) using PSV software. First, the device was tested for its resonant frequency and its mode of operation using Laser Doppler Vibrometry (LDV) with objective of testing the sensor in the presence of magnetic field. Initially a DC bias of 3 V using voltage source (Agilent B2961A) at top anchor and AC signal (periodic chirp) of 10 mV using the internal generator of LDV was applied to the resonant sensor's bottom electrodes and mode shape of the structure was observed for its motion at resonant frequency. The device was designed for its first and second mode of operation for both outer and inner gimbal respectively. Fig. 4 and Fig 5 depict the first and second mode of operation for device respectively. Device has its first and second resonant modes at 107.5 kHz and 187.25 kHz.

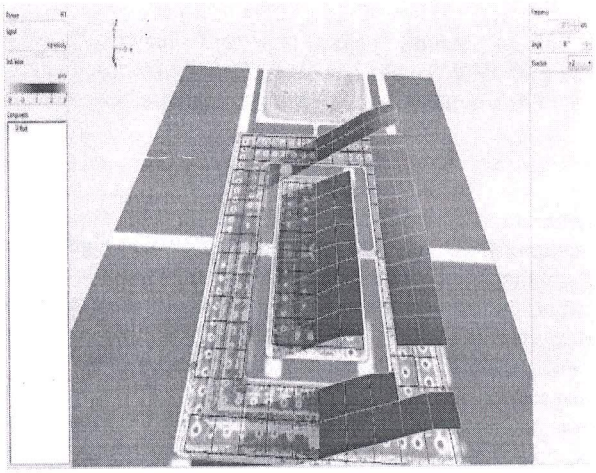

Fig. 4. First mode of vibration, measured using LDV (at ~107 kHz.)

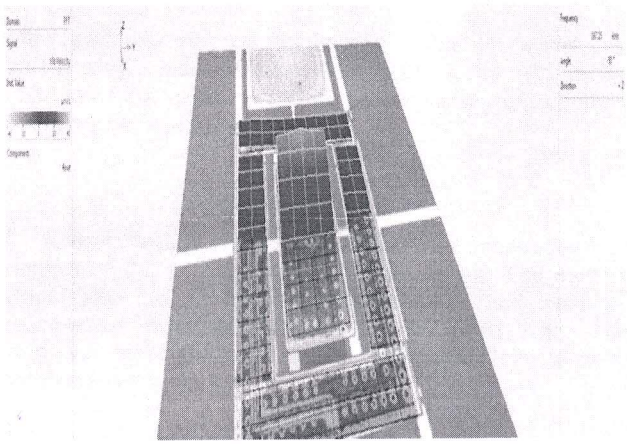

Fig. 5. Second mode of vibration, measured using LDV (at ~187 kHz.)

In order to see the effect of magnetic field, the frequency response of sensor is compared when no magnetic field is applied and vis-a-vis when external magnetic field is applied. A sinusoidal excitation current is applied in between the coil extreme ends i.e. at the anchors by applying voltage at one end and ground at the other. Current was applied in the coil, with a frequency sweep. Also, the bottom electrodes for the inner and outer gimbal are grounded. Then, the frequency response of the sensor is measured. Thereafter magnetic field of 120 Gauss is applied from a permanent magnet and frequency response is measured. For outer gimbal the current is in x-direction and magnetic field applied in y-direction. Also, Fig.6 illustrates the resonant frequency response of the torsional magnetometer for outer gimbal in presence and absence of magnetic field and with applied current of 0.1 mA. For, inner gimbal the current is in y direction, so a magnetic field of 120 Gauss is applied in x-direction. This resulted in a Lorentz force transduction deflecting the inner gimbal in torsional mode.Fig.7 illustrates the resonant frequency response of the torsional magnetometer for inner gimbal in presence and absence of magnetic field and with applied current of 0.1mA. The offset is due to electrostatic excitation, while the bottom electrode is grounded, but it is significantly lower w.r.t. to the magnetic field response of the sensor. The quality factor of the sensor was ~8.15 and ~2.70 along y and x axis respectively.

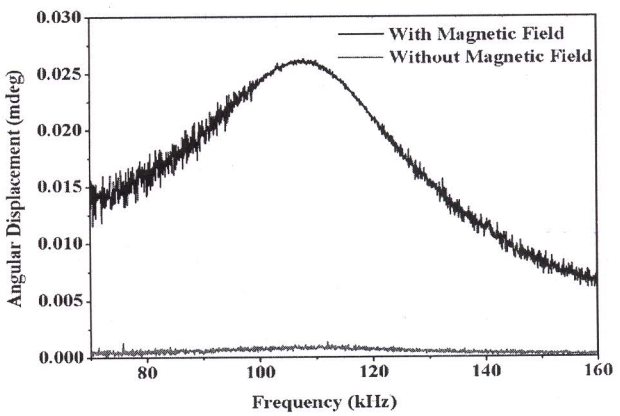

Fig.6. Frequency response of the resonator along x-axis showing the amplitude plot

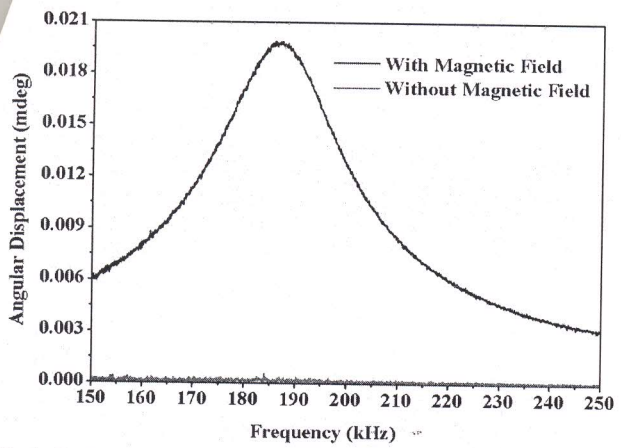

Fig.7. Frequency response of the resonator along y-axis showing the amplitude plot

Thus the device was tested for its operation as a Lorentz force MEMS magnetometer using silicon as structural layer with dual axis sensing. The tests were carried out at atmospheric pressure. For improving the response of the sensor, it needs to be vacuum packaged. The response is also limited by noise. The noise in the sensors mechanical output is mainly due to Brownian noise from the MEMS structure. The Brownian noise density is given by [13],

$$F_B = \sqrt{4k_bT\frac{k}{2\pi f_n Q}} \quad [\frac{\mathrm{N}}{\sqrt{\mathrm{Hz}}}] \qquad (3)$$

Where k_b is Boltzmann's constant, $T$is temperature in degree Kelvin, and k is the spring constant, f_n is the resonant frequency and Q is the quality factor, N_L is the number of loop and L being effective length. For torsional resonator k is calculated by dividing the torsional stiffness with square of average torque arm (for small tilting angle). The theoretical Brownian noise limited resolution of the sensor is given by [14],

$$B_B = \frac{2*F_B}{N_L(Li)} \quad [\frac{\mathrm{T}}{\sqrt{\mathrm{Hz}}}] \qquad (4)$$

The theoretical Brownian noise limited resolution calculated reaches to 119 nT/ $\sqrt{}$ Hz and 430 nT/ $\sqrt{}$ Hz for y and x magnetic field sensing, calculated at 1mA current and with Q of 3000.

V. CONCLUSIONS

We demonstrate a dual-axis Lorentz force magnetometer using a single resonating structure. The two DOF torsional gyroscope structure has been utilized for the development of x and y axis magnetic field sensor. The device responds to the external magnetic field applied in both x and y direction. It was tested for Lorentz force transduction at ambient pressure with resonant modes at 107 kHz and 187 kHz. The device can detect magnetic field in two directions. The sensor was developed using anodic bonding technique with silicon as structural layer, which is relatively simple to realize and requires low temperature (<400°C) processes. Future work should, therefore, include development of the structure such that the resonant modes are designed to be very close to each other, such that with one frequency of excitation current, two axis sensing is made possible. Also, better vacuum packaging (10 Pa) of the structure and its capacitive sensing circuitry would be worked upon.

ACKNOWLEDGMENT

Authors would like to acknowledge the motivation and support of the Director, CSIR-CEERI, Pilani. The authors would also like to thank all the scientific and technical members of Smart Sensors Area at CSIR-CEERI, Pilani. The work was financially supported by CSIR, New Delhi, to carry out the research work.

REFERENCES

[1] V. Kumar, A. Ramezany, M. Mahdavi, and S. Pourkamali, "Amplitude modulated Lorentz force MEMS magnetometer with picotesla sensitivity," *Journal of Micromechanics and Microengineering*, vol. 26, no. 10, p. 105021, Oct. 2016.

[2] Herrera-May, Agustín L., Luz A. Aguilera-Cortés, Pedro J. García-Ramírez, Nelly B. Mota-Carrillo, Wendy Y. Padrón-Hernández, and Eduard Figueras, "Development of resonant magnetic field microsensors: challenges and future applications", In *Microsensors*. IntechOpen, 2011.

[3] K. Sinha and M. Tabib-Azar, "27 pT Silicon Nitride MEMS Magnetometer for Brain Imaging," *IEEE Sensors Journal*, vol. 16, no. 17, pp. 6551–6558, Sep. 2016.

[4] M. Y. Elsayed, P.-V. Cicek, F. Nabki, and M. N. El-Gamal, "Surface Micromachined Combined Magnetometer/Accelerometer for Above-IC Integration," *Journal of Microelectromechanical Systems*, vol. 24, no. 4, pp. 1029–1037, Aug. 2015.

[5] J. Kyynäräinen*et al.*, "A 3D micromechanical compass," *Sensors and Actuators A: Physical*, vol. 142, no. 2, pp. 561–568, Apr. 2008.

[6] A. Herrera-May, J. Soler-Balcazar, H. Vázquez-Leal, J. Martínez-Castillo, M. Vigueras-Zuñiga, and L. Aguilera-Cortés, "Recent Advances of MEMS Resonators for Lorentz Force Based Magnetic Field Sensors: Design, Applications and Challenges," *Sensors*, vol. 16, no. 9, p. 1359, Aug. 2016.

[7] S. Pala, M. Cicek, and K. Azgin, "A Lorentz force MEMS magnetometer," in 2016 IEEE SENSORS, Orlando, FL, USA, 2016, pp. 1–3.

[8] Aditi, Gopal, Ram. "Fabrication of MEMS xylophone magnetometer by anodic bonding technique using SOI wafer," *Microsystem Technologies* vol.23, no. 1, pp.81-90, 2017.

[9] L. Wu, Z. Tian, D. Ren, and Z. You, "A Miniature Resonant and Torsional Magnetometer Based on Lorentz Force," *Micromachines*, vol. 9, no. 12, p. 666, Dec. 2018.

[10] D. Ren, L. Wu, M. Yan, M. Cui, Z. You, and M. Hu, "Design and Analyses of a MEMS Based Resonant Magnetometer," *Sensors*, vol. 9, no. 9, pp. 6951–6966, Sep. 2009.

[11] C. R. Marra, M. Gadola, G. Laghi, G. Gattere, and G. Langfelder, "Monolithic 3-Axis MEMS Multi-Loop Magnetometer: A Performance Analysis," Journal of Microelectromechanical Systems, vol. 27, no. 4, pp. 748–758, Aug. 2018.

[12] M. Li *et al.*, "Single-structure 3-axis Lorentz force magnetometer with sub-30 nT/√HZ resolution," in *2014 IEEE 27th International Conference on Micro Electro Mechanical Systems (MEMS)*, San Francisco, CA, USA, 2014, pp. 80–83.

[13] V. T. Rouf, M. Li, and D. A. Horsley, "Area-Efficient Three Axis MEMS Lorentz Force Magnetometer," *IEEE Sensors Journal*, vol. 13, no. 11, pp. 4474–4481, Nov. 2013.

[14] C. R. Marra, M. Gadola, G. Laghi, G. Gattere and G. Langfelder, "Monolithic 3-Axis MEMS Multi-Loop Magnetometer: A Performance Analysis," in Journal of Microelectromechanical Systems, vol. 27, no. 4, pp. 748-758, Aug. 2018.